Review

Rational Design of Nanostructured MnO_2 Cathode for High-performance Aqueous Zinc Ion Batteries

LI Qi[1], ZHAO Yajun[1], WANG Yueyang[1], Abdalla Kovan KHASRAW[1], ZHAO Yi[1,2]✉ and SUN Xiaoming[1]✉

Received May 16, 2023
Accepted July 5, 2023
© Jilin University, The Editorial Department of Chemical Research in Chinese Universities and Springer-Verlag GmbH

Aqueous Zn-MnO_2 batteries hold a promising potential for grid-scale energy storage applications due to their intrinsic safety, low fabrication cost, environmental friendliness and high theoretical energy densities. Developing novel nanostructured cathode materials with high discharge voltage, large capacity and excellent structural stability is one of the critical ways to achieve the high-performance aqueous Zn batteries. Enlighten by that, comprehending principles of materials design and identifying the challenges faced by the state-of-the-art MnO_2 hosts are vital preconditions. Rather than a simple comparison, this review mainly focuses on design strategies regarding to MnO_2-based materials, including defect engineering, interfacial engineering, and pre-intercalation engineering. In addition, the energy storage mechanisms of MnO_2-based cathodes are discussed to clarify the complicated chemical reactions during battery cycling. Challenges and perspectives are outlined to guide the further development of advanced Zn-MnO_2 batteries.

Keywords Aqueous Zn battery; Nanostructured MnO_2 cathode; Energy storage mechanism; Material design strategy

1 Introduction

In recent years, aqueous zinc ion batteries(AZIBs) have gained tremendous attention due to their advantageous properties, such as non-flammability, non-toxicity, and high ionic conductivity[1,2]. In addition, the fabrication process of AZIBs is relatively simple and economically feasible, meeting the present strategic demands for sustainable development. However, conventional alkaline Zn batteries, such as Zn-Mn, Zn-Ni, and Zn-air batteries generally suffer from severe side reactions associated with dendrites formation, corrosion, and hydrogen evolution, leading to unsatisfactory performance. To mitigate these issues, massive research efforts have been devoted to developing AZIBs with novel electrode materials and mild aqueous electrolytes have been studied for Zn batteries. Manganese-based oxides, vanadium-based oxides, Prussian blue analogs and organic compounds have been developed as cathodes for aqueous Zn batteries. Among them, MnO_2-based cathode materials have attracted much attention due to their promising electrochemical performance with high energy density and multi-electron transfer reactions[3−5]. Yet, their development and practical application have been hindered by the critical problems of low intrinsic electronic conductivity as well as unwanted irreversible phase transformation, causing inferior rate capability and fast capacity decay[6−8]. Considering escalating energy demand and growing interest in AZIBs, it is urgent to break the bottleneck of Mn-based cathode with high capacity, fast redox kinetics, and long cycling life.

Researchers have employed various modification strategies to develop the electrochemical performance of Mn-based hosts, such as defect engineering, interfacial engineering, and pre-intercalation engineering, as displayed in Fig.1[9]. These strategies significantly contribute toward the enhancement in electrochemical performance of Zn-MnO_2 batteries. Defect engineering, involving heteroatoms doping and creating defects, is the most commonly used strategy in tailoring the electronic properties and structural stability of MnO_2, leading to improved rate/cycling performance[10,11]. Moreover, interfacial engineering serves as an alternative strategy to enhance the structural stability of MnO_2, in a way of prohibiting serious side reactions and Mn dissolution problems[12]. Furthermore, pre-intercalation engineering has emerged as an effective approach to improving the battery performance by increasing the interlayer spacing of MnO_2. Generally, guest species, including water molecules, metal/non-metal ions, as well as inorganic/organic molecules, can intercalate into the host framework and decrease the electrostatic interactions with inserted Zn ions, resulting in stabilized inherent structure of MnO_2[13]. Besides, researchers have developed size-dependent and morphology-controlled approaches to manipulating charge distribution and electrode kinetics in MnO_2 hosts. By shortening the ion diffusion path and increasing the surface area of the electrode, Zn-MnO_2 batteries exhibit good rate capability and high energy storage performance[9].

To date, considerable progress has been made on the

✉ SUN Xiaoming
sunxm@mail.buct.edu.cn
✉ ZHAO Yi
zybattery@buct.edu.cn
1. State Key Laboratory of Chemical Resource Engineering, College of Chemistry, Beijing University of Chemical Technology, Beijing 100029, P. R. China;
2. Advanced Technology Research Institute, Beijing Institute of Technology, Jinan 250300, P. R. China

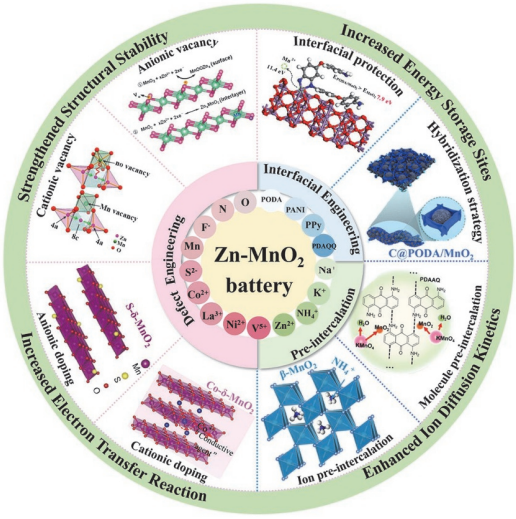

Fig.1 Rational design strategies to enhance the electrochemical performance of nanostructured MnO_2 cathode *via* defect engineering, interfacial engineering and pre-intercalation engineering

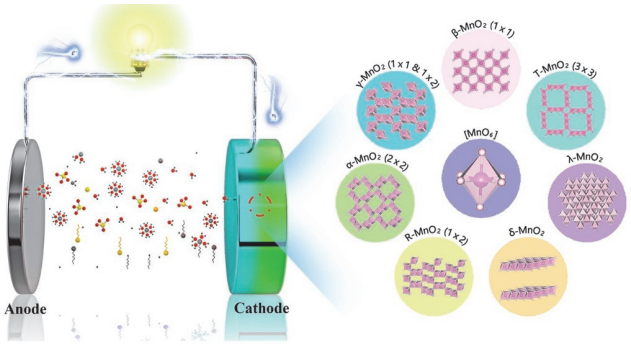

Fig.2 Crystal structures of various MnO_2 cathodes including *α*-MnO_2, *β*-MnO_2, *γ*-MnO_2, *δ*-MnO_2, *λ*-MnO_2, T-MnO_2(Todorokite-type) and R-MnO_2(Ramsdellite-type) for aqueous Zn-MnO_2 batteries

modification strategies for promoting the development of MnO_2 cathode and discovering related energy storage mechanisms. As a result, an up-to-date review is necessary to systematically summarize the latest achievement of modification strategies for MnO_2 cathode. By examining the recent progresses of theoretical and experimental investigations, this review provides a systematic and thorough survey aiming at optimizing crystal structure and clarifying energy storage mechanisms of MnO_2 cathode. Finally, the review concludes with prospects for future research and development of high-performance MnO_2 cathodes based on a novel chemical reaction design for next-generation batteries.

2 Crystal Phases of Nanostructured MnO_2

MnO_2 hosts exhibit available rich redox chemistry(Mn^{2+}, Mn^{3+}, Mn^{4+}) and form a large variety of tunnel or layered polymorphs(*α*-, *β*-, *γ*- ,*δ*-, *λ*-, R- and T-)[14−21], which depend on sharing vertices/edges of basic building unit[MnO_6] octahedra[22−24]. To better understand MnO_2 materials applied in AZIBs, we summarize different crystal structures of MnO_2 as described below(Fig.2). Specifically, *α*-MnO_2(hollandite-type) has a typical (2×2) tunnels structure, which is composed of double chains in the plane by corner-sharing of [MnO_6] octahedra. Different predominant cations existing in its tunnel structure, such as Ba, Na, K and Pb enable *α*-MnO_2 with a large tunnel size(*ca*. 4.6 Å, 1 Å=0.1 nm)[25]. *β*-MnO_2 (pyrolusite-type) has (1×1) tunnel along the *c* axis composed of single chains by vertical-sharing of [MnO_6] octahedral. Hence, *β*-MnO_2 has the narrowest tunnel size(*ca*. 1.89 Å) compared with other types polymorphs MnO_2, which is difficult for ions diffusion(Li^+, Zn^{2+}) into its structure[16]. In contrast, R-MnO_2 (ramsdellite-type) contains (1×2) tunnels, formed by sharing corners of one double chains in parallel direction and another in vertical direction. The structure of *γ*-MnO_2(nsutite-type) is randomly comprised of tunnels with (1×1) and (1×2), normally regarded as an intergrowth of *β*-MnO_2 and R-MnO_2. *λ*-MnO_2 is composed of [MnO_6] octahedra connected with [MnO_4] tetrahedral. The Mn^{2+} and Mn^{3+} occupy the tetrahedral and octahedral sites, respectively[26]. T-type(todorokite-type) MnO_2 has (3×3) tunnel structures, which are made of large edge-sharing [MnO_6] octahedra panel cross sections since it is constructed of triple chains composed of [MnO_6] octahedra. *δ*-MnO_2(layered-type) is constructed by sheets of edge sharing [MnO_6] octahedra. Unlike tunneled MnO_2, cations and/or water molecules can act as “pilar” to maintain layered structure of MnO_2, which can boost the ion diffusion and cycling performance of Zn-Mn batteries.

Furthermore, much effort has been devoted to the preparation of low-dimensional MnO_2 nanostructures with diverse polymorphs. For example, *α*-, *β*- and *γ*-MnO_2 have been synthesized into various shapes(such as nanowires, tubes, sheets, etc.) through different synthesis methods and controlled reaction conditions. And the properties and performances of MnO_2 are generally influenced by their morphology and dimensions. Therefore, most MnO_2 cathodes with various crystal types are generally modified with nanostructured morphologies to enhance the reactive sites and improve the redox kinetics[27]. Currently, there are four main types of nanostructured MnO_2: zero-dimensional(0D), one-dimensional(1D), two-dimensional(2D) and three-dimensional(3D) nanomaterials. As for 0D nanomaterial (such as nanodots), Zhu *et al*.[6] reported the high capacity and ultra-stable Zn-Mn batteries by using *δ*-MnO_2 nanodots as the cathode, as shown in Fig.3(A). As for 1D nanomaterials (such as nanorods, nanowires, nanofibers and nanotubes), Chen *et al*.[28−32] employed *γ*-MnO_2 nanowires and nanotubes

https://doi.org/10.1007/s40242-023-3126-x

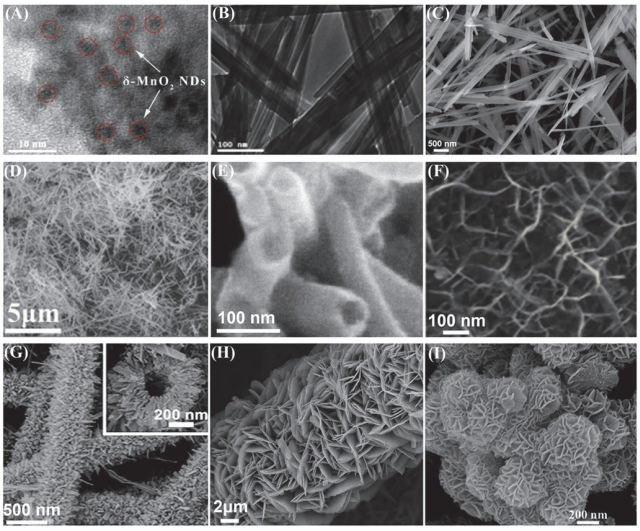

Fig.3 TEM and SEM images of nanostructured MnO_2

(A) The δ-MnO_2 nanodots; (B) the α-MnO_2 nanowires; (C) the β-MnO_2 with rich oxygen defects nanorods; (D) the γ-MnO_2 nanorods; (E) the γ-MnO_2 nanotubes; (F) the ε-MnO_2 Sponge-like nanostructure; (G) the K^+-doped α-MnO_2 nanotubes; (H) the Co-doped δ-MnO_2 nanosheets; (I) the α-MnO_2 flowerlike nanospheres. (A) Reprinted with permission form Ref.[6], Copyright 2022, Elsevier; (B, D) reprinted with permission form Ref.[28], Copyright 2006, American Chemical Society; (C) reprinted with permission from Ref.[29], Copyright 2020, Elsevier; (E) reprinted with permission from Ref.[30], Copyright 2005, Wiley-VCH; (F) reprinted with permission from Ref.[31], Copyright 2009, Royal Society of Chemistry; (G) reprinted with permission from Ref.[32], Copyright 2012, Royal Society of Chemistry; (I) reprinted with permission from Ref.[33], Copyright 2010, American Chemical Society.

as the cathode for significantly improving the battery performance of AZIBs, as displayed in Fig.3(B)—(G). A regular nanosheet structure of Co-doped MnO_2 was synthesized by our group, by which the ion diffusion rate was greatly increased in Fig.3(H). To further increase the specific surface of MnO_2, Dong *et al.*[33] fabricated δ-MnO_2 nanosheets for enhancing the redox kinetics and zinc storage capacity of Zn-Mn devices, as displayed in Fig.3(I). Besides, flower-shaped MnO_2 nanosheets have been used as high-performance cathodes to greatly improve the capacity and stability of Zn-Mn devices[32]. Therefore, both the crystal structure and morphology of MnO_2 have an impact on enhancing the performance of aqueous Zn batteries.

3 Design Strategies on MnO_2 Cathode

Various crystal structures and multiple valence states can endow MnO_2 electrodes with sufficient theoretical specific capacity and high working voltage. However, MnO_2 cathodes are still challenged by poor rate performance, inferior rate capability, and fast capacity decay caused by their poor electronic conductivity, inevitable Mn dissolution, and dramatic volume changes[34−36]. It is of significance to improve the electrochemical performance of MnO_2 cathodes by reasonable design strategies for AZIBs. The modification strategies are described in detail in the following three sections.

3.1 Defect Engineering

Defect engineering has been recognized as a common strategy to manipulate the physical and chemical properties of the hosts. Specifically, defect engineering has been extensively applied in manipulating MnO_2 cathode for significantly improved capacity, cycle stability and rate performance[37]. As the most acknowledged defect engineering, vacancies and doping have been utilized to enhance the electrochemical performance of Mn-based materials[38−40]. This section summarizes the latest discussions on defect engineering for MnO_2 cathode materials, including anionic and cationic vacancies and doping.

3.1.1 Vacancy Defects

Oxygen vacancies, as the most common defects, can tune the surface property and electronic distribution of Mn-based materials without introducing impurities and affecting the geometrical structure, resulting in improved adsorption energy of Zn^{2+} and electronic conductivity of MnO_2 materials[as shown in Fig.4(A)][41]. Nevertheless, pristine MnO_2 exhibits more thermodynamical stability for inserted Zn ions due to the strong chemical bond between Zn and O, hindering the reversible insertion/extraction of zinc ions[42,43]. To boost the diffusion kinetics of Zn ions, Xue *et al.*[10] synthesized an oxygen-deficient δ-MnO_2 cathode with a large specific capacity of 345 $mA{\cdot}h{\cdot}g^{-1}$ at 0.2 A/g and a superior rate performance. It is attributed that the oxygen vacancies in MnO_2 provide more surface capacitive contribution by increasing the active surface and processing more electrons for delocalizing into the electrode[15]. Besides, Kang *et al.*[44] prepared oxygen defect-rich MnO_2(O-MnO_2) nanosheets for enhancing the electrical conductivity and Zn ion storage capacity. Mai *et al.*[21] rationally designed Ti-doped α-MnO_2 nanowires with oxygen vacancies. Moreover, the oxygen vacancies can open [MnO_6] octahedral walls and generate a local electric field, accelerating ion/electron migration kinetics for high-rate Zn ion storage.

In addition to anionic vacancy, it has been recognized that cationic vacancies also can effectively tune the electronic structure of MnO_2 to reduce the charge transfer resistance and enhance electrode kinetics. Also, such vacancies can be used as extra active sites to store more cation ions, increasing energy storage capability for electrode materials[45]. Chao *et al.*[46] have successfully prepared Mn vacancy containing MnO_2(V_{Mn}-MnO_2) for an electrolytic Zn-MnO_2 system in Fig.4(C). According to theoretical calculations, the increased surface electron density on the Mn vacancies can promote the zinc ion storage performance with a lower energy barrier in V_{Mn}-MnO_2.

https://doi.org/10.1007/s40242-023-3126-x

To better unveil the positive effect of oxygen vacancies, experimental analyses and theoretical calculations can be combined to investigate the vacancies structure-function relationship[29].

3.1.2 Anionic Doping

Due to the strong electrostatic interaction between the electronegative of O atom and inserted Zn^{2+}, pristine MnO_2 shows a thermodynamically favorable attraction to Zn ions. Hence, the substitution of O atoms with a lower electronegative element can reduce the strong interaction of Zn—O bonds and improve Zn diffusion kinetics in MnO_2 cathode. Anionic doping is one of the most widely adopted strategies to introduce many interesting properties to cathode materials[11]. Specifically, the oxygen anion sites in MnO_2 could be partially replaced by non-metal elements, such as S^{2-}[42], N^{3-}[47]or F^-[48], which could change the intrinsic electronic structure and improve its electrochemical performance. Herein, we summarize the latest anion doping approaches, revealing the intrinsic mechanisms of doped anion.

Recently, Sun and co-workers[42] reported that the S doped MnO_2(S-MnO_2) cathode displayed large Zn storage capacity, high rate performance, and long cycling life. Combined with experiment results and theoretical studies, doped S anions can effectively enhance the intrinsic electronic conductivity of MnO_2 by narrowing its band gap, and accelerate reaction kinetics by weakening the electrostatic interactions between host and Zn^{2+} cations, as displayed in Fig.4(B). Besides, amorphous surfaces with rich oxygen defects on S-MnO_2 are formed during the preparation process, which provides extra active sites for more Zn ions storage with pseudocapacitive behavior[42]. Huang *et al.*[47] prepared a N-doped *ε*-MnO_2 (MnO_2@N) cathode and found the greatly improved conductivity and stability for MnO_2@N based Zn batteries. The improved electrochemical performance can be attributed to the formed Mn—N bonds for elongating the Mn—O bond and promoting the insertion of Zn^{2+}/H^+. Furthermore, N-doped MnO_2 can effectively reduce the electrostatic repulsion between the cathode and the inserted cations, such as Zn^{2+}/H^+ ions, and improve the electrode kinetics[48].

Moreover, Kim *et al.*[49] reported fluorine doped *β*-MnO_2 (F-MnO_2) cathode with a hierarchical structure *via* efficient defect engineering for improved ion insertion and transport kinetics of Zn-MnO_2 battery. On account of its similar ionic radii, O^{2-} can be efficiently replaced by F^- in F-MnO_2 for the enhanced electrical conductivity and energy-storing performance. Despite anionic doping has been proven as an

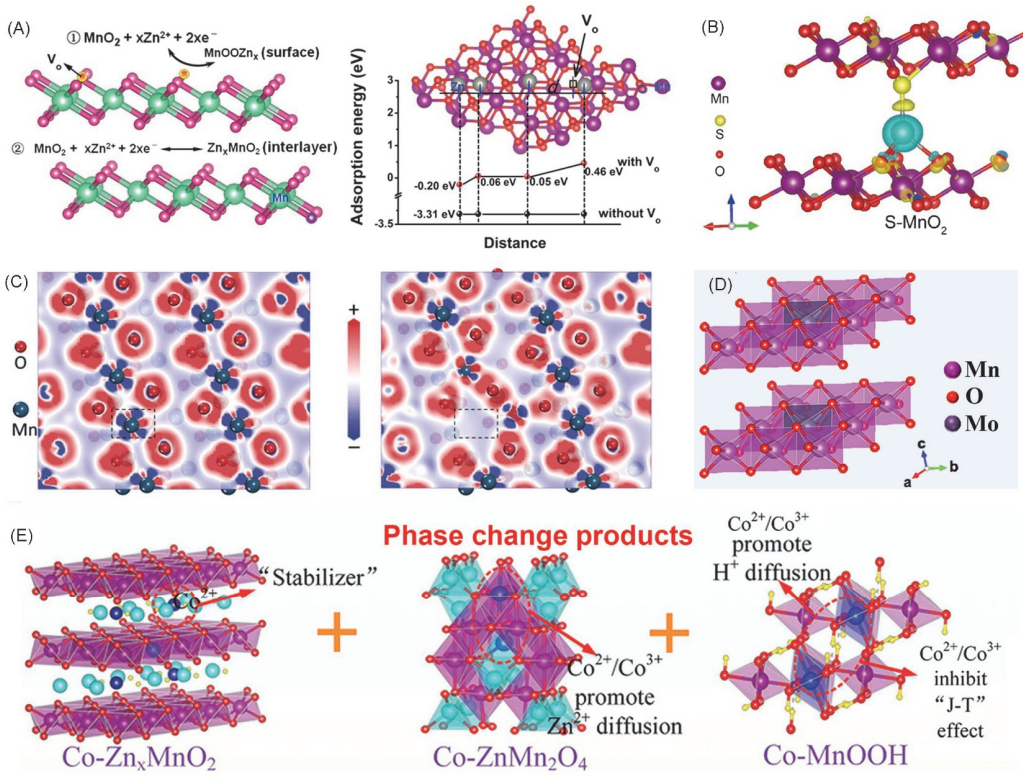

Fig.4 Structural schematics and reaction mechanisms of modified MnO_2 *via* defect engineering

(A) Mechanisms of oxygen-deficient *δ*-MnO_2 for Zn ions storage, and the calculated adsorption energies; (B) charge density difference distribution for Zn^{2+} inserted S-MnO_2; (C) electron density difference comparison of vacancy-free and Mn vacancy MnO_2; (D) the atomic structure of Mo-doped MnO_2; (E) phase change products of Co-doped MnO_2 after few cycles.

(A) Reprinted with permission form Ref.[41], Copyright 2019, Wiley-VCH; (B) reprinted with permission form Ref.[42], Copyright 2022, Elsevier; (C) reprinted with permission from Ref.[46], Copyright 2019, Wiley-VCH; (D) reprinted with permission from Ref.[55], Copyright 2022, Springer Nature; (E) reprinted with permission from Ref.[54] , Copyright 2020, Wiley-VCH.

https://doi.org/10.1007/s40242-023-3126-x

effective strategy for adjusting intrinsic electronic structures of MnO_2 cathodes, the battery performance is still unsatisfactory for superb AZIBs. More importantly, the anion doping effect regarding the structural change and energy storage performance of MnO_2 cathodes lacks in-depth exploration. Therefore, an anionic doping strategy can offer the direction for further exploration in cathode materials modification.

3.1.3 Cationic Doping

In addition to anionic doping, the effect of cationic doping for MnO_2 design is extraordinarily effective at enhancing the energy storage of MnO_2 cathode. The cathodes of AZIBs can show high electronic conductivity and better electrochemical behaviors by cationic doping to release the electrochemical activity potential of MnO_2. At present, many studies on cationic doping have been reported. The doping cations(such as V, K, Co, Ag, La, Na, Zn, Cu and H) not only show the common advantages, but also exhibit its particularity of each element[50−53]. Ji *et al.*[54] reported a MnO_2 cathode doped with multivalent cobalt ion for high-performance Zn-MnO_2 batteries. Specifically, doped Co^{2+}, Co^{3+} and Co^{4+} can act as a "interlay pillars" and "structural stabilizers", respectively, for the high capacity and stable MnO_2 cathodes, as shown in Fig.4(E)[54]. Recently, our group[55] studied the doping effect of high-value element in Mo^{5+} doped MnO_2, as displayed in Fig.4(D). It is worth noting that doped Mo^{5+} can not only improve the electronic conductivity, but also promote Jahn-Teller distortion of the octahedron [MnO_6] in $ZnMn_2O_4$, which further realizes the two-electron transfer of Mn^{2+}/MnO_2 to achieve an excellent performance of Zn-MnO_2 battery. Besides, dual cation doping enables to improve the capacity and rate performance of MnO_2 cathodes simultaneously. Hu *et al.*[56] reported co-doped of Ti/Ni-MnO_2 host for high-performance Zn batteries. Specifically, multivalent Ti ions could allow valence variation for a higher specific capacity and doped-Ni ions could regulate the proton transfer behavior in MnO_2 cathode. Thus, Mn-based cathodes doped with multivalent and hypervalent ions will provide a fillip for developing superb AZIBs.

3.2 Interfacial Engineering

Besides the doping effect, interfacial modification of MnO_2 composited with carbon materials and conductive polymers is being studied in depth for inhibiting the Jahn-Teller effect and inducing additional active sites, respectively. Two main strategies of hybridization and organic protection have been summarized in detail.

3.2.1 Hybridization Strategy

Low intrinsic electronic conductivity is the key issue for the development and practical application of Mn-based cathodes. Beyond defect engineering, hybridizing with conducting materials to construct composites is an effective way to improve the rate performance and stability of Zn-MnO_2 devices[57]. Currently, carbon materials modified by MnO_2 includes carbon cloth, carbon nanotubes(CNTs), super P, graphene nano flakes(CNFs), porous carbon and carbon boll, which have been reported as cathodes for AZIBs in Fig.5(B)[58−62]. Previously reported hybridization strategy is only a simple physical contact between the active MnO_2 and the carbon material, which increases contact resistance and results in unsatisfactory electrochemical performance[63]. Hence, it is urgent to explore MnO_2 hybrids with both enhanced conductivity and ion diffusion kinetics[64−67].

Recently, Tong *et al.*[68] prepared oxygen vacancy MnO_2 loaded on the carbon nanotubes(Vo-MnO_2/CNTs) as the cathode, in which CNTs with good electrical conductivity can greatly reduce charge transfer resistance of MnO_2, benefiting for superior rate capacity in Zn-MnO_2 devices[69]. Besides, carbon materials can prevent structural degradation and improve the cycling stability of MnO_2[70,71]. Zhao *et al.*[72] reported that the hybrid formation of Mn—O—C bonds between nanoporous carbon matrix and MnO_2 can efficiently inhibit Mn dissolution to strengthen the structural integrity of the composite cathode materials, as shown in Fig.5(A). In addition, carbon cloth is also a common carbon substrate, which can effectively facilitate the deposition process by providing nucleation sites to boost *in-situ* growth and conductivity of MnO_2 as illustrated in Fig.5(C)[73]. Hence, hybridization strategy can endow better electrochemical performance if new carbon materials are found.

3.2.2 Interfacial Protecting

Additionally, MnO_2, which is prone to structural collapsibility can be interfacial protected by organics to form stable organic-inorganic hybrids for advanced Zn batteries. Electrode materials have been coated with organics to prevent structural collapse, thus improving the stability and durability of lithium-ion batteries[74,75]. Similarly, it has been applied in organic/MnO_2 cathodes for AZIBs in recent years[7,8,12,76,77]. Very recently, Zhao *et al.*[72] reported a novel carbon-based poly(4,4'-oxybisbenzenamine)/MnO_2(denoted as PODA/MnO_2) hybrid cathode, in which MnO_2 was half-coated by PODA nanosheets to provide additional active sites and boost reaction kinetics. More importantly, Mn—N bonds formed between the interface of PODA and MnO_2 can greatly inhibit the

https://doi.org/10.1007/s40242-023-3126-x

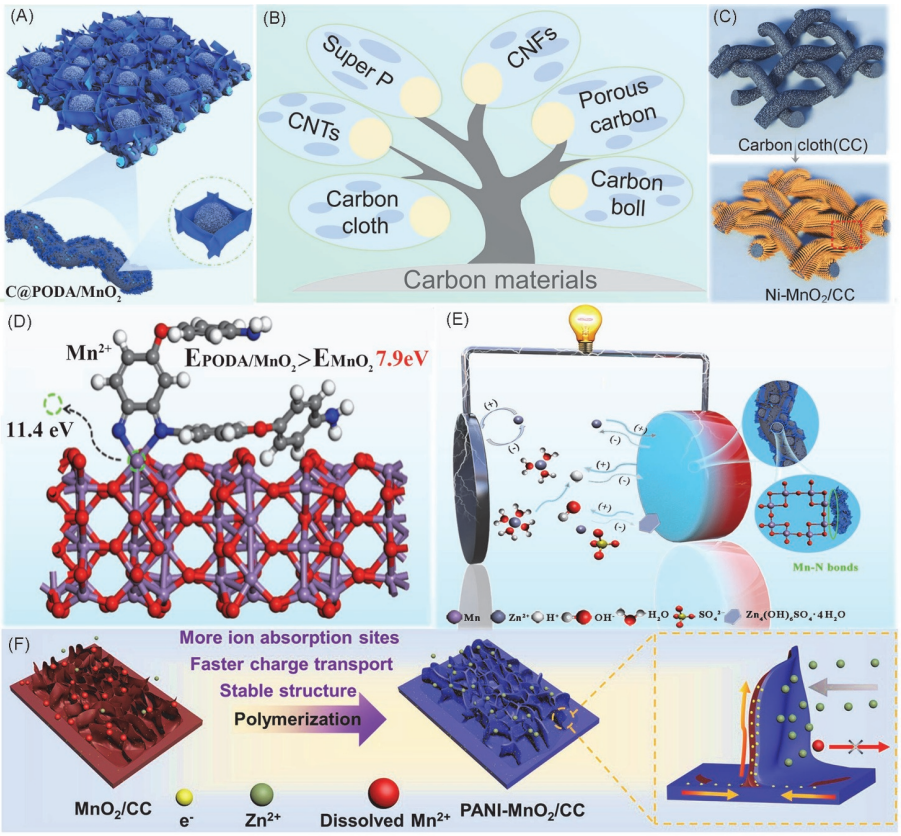

Fig.5 Structural design of MnO_2 hosts *via* interfacial engineering

(A) MnO_2 nanospheres half-wrapped by PODA nanosheets onto nanoporous carbon; (B) MnO_2 hybridized with carbon materials for enhanced structural integrity; (C) schematic diagram of *in-situ* growth Ni-doped MnO_2 onto carbon cloth; (D) energy barrier of Mn atom removed from the C@PODA/MnO_2; (E) interfacial protect mechanism of PODA/MnO_2 *via* newly formed Mn-N bond; (F) schematic illustration of the interfacial engineering of PANI-MnO_2/CC to form PANI protective/active layers with 3D network-like interfaces onto MnO_2.

(A, D, E) Reprinted with permission form Ref.[72], Copyright 2022, Wiley-VCH; (C) reprinted with permission form Ref.[73], Copyright 2022, Wiley-VCH; (F) reprinted with permission from Ref.[78], Copyright 2021, Elsevier.

dissolution of Mn atoms and inhibit the Jahn-Teller effect, improving the stability of PODA/MnO_2 hybrid in Fig.5(D). Hence, the energy storage capacity and structural integrity of MnO_2 can be enhanced by interfacial protection as displayed in Fig.5(E)[72].

Furthermore, polyaniline(PANI), poly(3,4-ethylenedioxy thiophene)(PEDOT), and polypyrrole(PPy), with flexible framework, also have been used for protecting the stability of MnO_2 cathodes. Ruan *et al.*[78] reasonably designed the three-dimensional networks of MnO_2-PANI hybrid *in-situ* deposited on carbon cloth(PANI-MnO_2/CC) for Zn ion storage in Fig.5(F). The hybrid cathode exhibits rapid ion diffusion ability and relatively stable structure due to the tight 3D mesh interfaces formed between the MnO_2, PANI and carbon cloth. Although organic protection provides a new idea for the structural integrity of MnO_2, it is worth noting that organic interfacial strategy is relatively rare in the design of high-performance of Zn-MnO_2 devices.

3.3 Pre-intercalation Strategy

In addition to defect engineering and interfacial engineering, the pre-intercalation strategy can also effectively improve the electrochemical performance of MnO_2 hosts[13]. Pre-intercalation strategy mainly aims at nanostructured MnO_2 by inserting a small amount of "guest materials" with activity or non-activity for enhanced electrochemical performance. Currently, guest materials mainly include metal ions, lattice water molecules and organic molecules. The influence of pre-intercalation effect on the chemical properties and energy storage mechanisms will be analyzed in this section.

3.3.1 Ion Pre-intercalation

Currently, inorganic cation intercalation has been widely used to expand the interlayer spacing and keep the crystal structural stability of MnO_2 electrodes[79]. Up to now, Na^+[38,80,81], Ag^+[82], Cu^{2+}[83,84], K^+[85,86] and Zn^{2+}[87] have been intercalated into MnO_2 hosts for speeding the commercialization of AZIBs. Yu *et al.*[88] reported a Na^+/crystal water co-intercalated layered MnO_2 cathode of $Na_{0.55}Mn_2O_4{\cdot}0.57H_2O$(NMOH) for high-performance AZIBs in Fig.6(B). Besides, the effect of enlarged interlayer spacing, pre-intercalated Na^+ can be substituted

with Zn^{2+} in the first cycle to further stabilize the layered MnO_2, resulting in exceptional specific capacity and satisfactory cycling lifespan of NMOH cathodes. Besides, intercalated K^+ acts as pillars, which have been reported in modified δ-MnO_2(denoted as KMO) to speed the sluggish ion diffusion in Fig.6(C)[89], resulting in high power capability of KMO cathode. It is worth noting that excessive pre-intercalated cations may lead to a phase transition from a two-dimensional layered structure to a one-dimensional tunnel structure, which can slow ion diffusion in the layered channel of MnO_2[90]. Parkin *et al.*[91] systematically revealed the threshold K/Mn ratio of 0.26 through DFT simulations for inhibiting the structural transition by stabilizing δ-MnO_2[Fig.6(D)]. In addition to alkali metals, Al^{3+} intercalated α-MnO_2(AMO) with stable cycling performance and superior rate capability was illustrated in Fig.6(A)[92].

Therefore, the ion pre-intercalation strategy plays an obvious role in improving the diffusion kinetics and cycling life of Mn-based cathodes[79]. Yet, the pre-intercalation content of ions should attract the attention of researchers for obtaining advanced Zn-Mn batteries. Specifically, a low ratio of intercalated ion cannot effectively increase the electrochemical performance of MnO_2 cathodes. Whereas, excessive cations can greatly reduce the specific capacity and even change the intrinsic structure MnO_2. Thus, it is particularly essential to select a suitable ratio of cation content for pre-intercalation strategy[93,94]. Moreover, pre-intercalation chemistry should be explored in-depth for the rational design of superb cathodes.

3.3.2 Molecule Pre-intercalation

Metal ions and water molecules can easily escape from the interlayer of MnO_2, leading to serious capacity decaying during the charging/discharging process[92]. To solve these issues, organic molecules with stable conjugated structures have acted as interlayer pillars of layered MnO_2. Guest materials of organics can not only stabilize the layered structure of MnO_2, but also endow extra redox groups for storing more Zn ions. Currently, organic molecules of aniline monomer[95], PANI[96], PEDOT[97] and PPy[98] have been reported for the modified MnO_2.

In 2015, Wang *et al.*[95] verified that aniline monomers could be intercalated into MnO_2 layers through experiments and DFT calculations. Based on this discovery, Wang *et al.*[96]

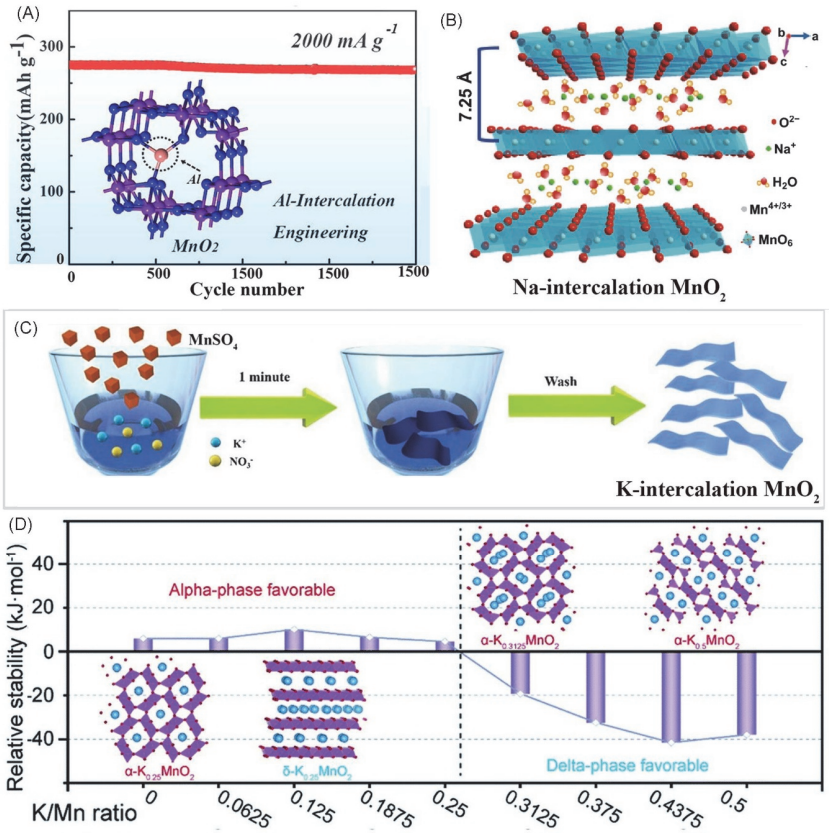

Fig.6 Ions pre-intercalation strategy for MnO_2 cathodes

(A) Al^{3+} pre-intercalated MnO_2 cathode for high cycling stability; (B) crystal structure of Na^+ pre-intercalated MnO_2 cathode with fast redox kinetics; (C) the fabrication process of K^+ pre-intercalated MnO_2; (D) the relative stability of delta phase to alpha phase as a function of K/Mn ratio *via* DFT simulation.

(A) Reprinted with permission form Ref.[92], Copyright 2021, Elsevier; (B) reprinted with permission form Ref.[88], Copyright 2020, Springer Nature; (C) reprinted with permission from Ref.[89], Copyright 2021, Wiley-VCH; (D) reprinted with permission from Ref.[91], Copyright 2020, Royal Society of Chemistry.

https://doi.org/10.1007/s40242-023-3126-x

prepared PANI-intercalated MnO_2 hybrids for the high-performance AZIBs through inorganic/organic interfacial reaction, as illustrated in Fig.7(B). Specifically, the chemical oxidative polymerization of aniline and the reduction reaction of MnO_4^{2-} facilitated the layered assembly of PANI-MnO_2. Due to the pre-intercalation effect, PANI-MnO_2 cathode displayed high capacity retention and a long lifespan even at high current density and deep discharge tests, respectively. On the basis of traditional organic molecules intercalation, quinones have attracted much attention due to their structural diversity and resource sustainability[99−102]. The intermolecular forces(such as van der Waals forces, π-π forces, etc.) can provide an elastic matrix for the reversible insertion/extraction of Zn^{2+}. Besides, inserted quinones can also facilitate the ion diffusion process in the adjustable interlayers of MnO_2[103−107]. Hence, the coupling inorganic MnO_2 and poly(1,5-diaminoanthraquinone)(MnO_2@PDAAQ) cathode exhibited a significantly enhanced capacity and cycling stability compared to the original MnO_2 and PDAAQ cathodes in Fig.7(A)[108]. Very recently, PEDOT pre-intercalated MnO_2 with regulated interlayer structure has been reported for constructing AZIBs[Fig.7(C)][97]. In conclusion, organic molecule intercalation can significantly improve the energy storage performance of MnO_2. Moreover, more novel intercalated organics with redox groups and stable structure can be developed for superb cathodes.

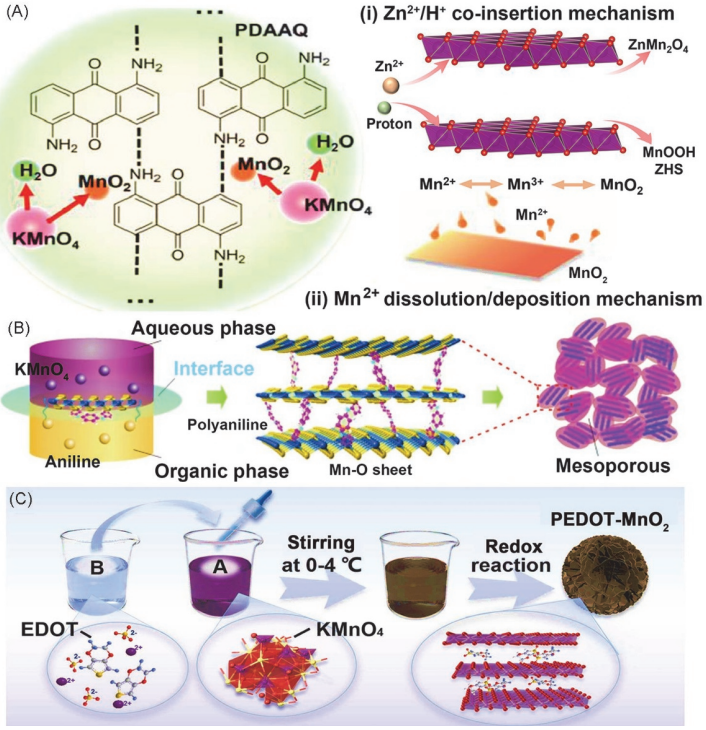

Fig.7 Schematic illustration of organic pre-intercalated MnO_2 cathodes

(A) PDAAQ pre-intercalated MnO_2 cathode for boosting the mechanisms of Zn^{2+}/H^+ co-insertion and dissolution/deposition reaction; (B) PANI pre-intercalated MnO_2 cathode for building high-capacity and long-lifespan Zn-MnO_2 battery; (C) PEDOT pre-intercalated MnO_2 cathode for speeding the ion diffusion.
(A) Reprinted with permission form Ref.[108], Copyright 2022, Elsevier; (B) reprinted with permission from Ref.[96], Copyright 2018, Springer Nature; (C) reprinted with permission from Ref.[97], Copyright 2023, Elsevier.

4 Energy Storage Mechanism of Mn-based Oxides

Although significant progress on MnO_2 cathode materials has been made in enhancing their electrochemical performance, the energy storage mechanism of MnO_2 cathode is more complex than that of other materials. According to the experimental experiences and theoretical calculations, energy storage mechanisms may be related to the polycrystalline types(α-, β-, γ-, δ-, λ-, R- and T-) and particle size of MnO_2 itself, as well as the acid-base variation of electrolyte[9,109,110]. So far, there are three mainstream energy storage mechanisms for MnO_2-based AZIBs: reversible ion insertion mechanism, conversion reaction mechanism and dissolution-deposition mechanism. This section provides detailed and deep discussions on energy storage mechanisms for the future investigation and construction of high-performance Zn-MnO_2 systems.

4.1 Reversible Ion Insertion Mechanism

The ionic radius of hydrated Zn^{2+}(4.12 Å) is comparable with that of hydrated Li^+(3.40 Å), which is favorable for Zn^{2+} intercalation/extraction into the host structure of MnO_2-based cathode materials. Kang *et al.*[111] suggested reversible

https://doi.org/10.1007/s40242-023-3126-x

storage/release of Zn ions into tunnels of α-MnO_2 cathode in $ZnSO_4$ electrolyte with the reversible formation of $ZnMn_2O_4$, confirming Zn intercalation/extraction energy storage mechanism for MnO_2-based cathodes. However, the storage mechanism of other types MnO_2-based cathode materials in neutral or mild acidic aqueous electrolytes remains controversial[20,112−114]. Although a similar zinc ions extraction behavior can be observed in ε-MnO_2 cathode, the insertion of Zn^{2+} cannot be completely reversible in the electrolyte of $ZnSO_4$ and $MnSO_4$[24]. Wang *et al.*[110] carried out electroanalytical technology to disclose the different mechanisms for electrodeposited ε-MnO_2 cathode. By using a combination of galvanostatic intermittent titration technique(GITT) and electrochemical impedance spectroscopy(EIS), it has been confirmed that H^+ ions are inserted into MnO_2 host structure at the higher voltage platform of 1.4 V, while Zn ions are inserted at the lower voltage platform of 0.6 V. Meanwhile, the continuously emerged equilibrium phases of MnOOH and $ZnMn_2O_4$ were obtained by electrochemical tests and *ex-situ* XRD analyses, which further supports the mechanism that MnO_2 cathode first underwent H^+ insertion and then Zn^{2+} insertion[Fig.8(A)][73].

Based on insertion-type mechanism, MnO_2 cathodes face structural instability issues of crystal collapse and Mn dissociation caused by the strong interaction between inserted ions and hosts. Therefore, rational structural design of constructing high stable host and fast ion diffusion is vital for Mn-based cathodes, especially for maintaining structural integrity and boosting redox kinetics during cycling tests.

4.2 Conversion Reaction Mechanism

Except for the Zn^{2+} intercalation chemistry, various conversion-type mechanisms based on reversible phase transformation of Mn-based cathodes have been reported during the energy storage process[113,115]. As reported, the polymorphs of α-MnO_2, β-MnO_2 and γ-MnO_2 usually undergo a phase transformation from tunneled into layered Zn-buserite after the first discharge process[109,116]. To confirm that, Chen *et al.*[19] constructed Zn-MnO_2 cells based on β-MnO_2 cathode, Zn anode and $Zn(CF_3SO_3)_2$ electrolyte with $Mn(CF_3SO_3)_2$ addictive. It was found that β-MnO_2 exhibited an irreversible phase transformation into Zn-buserite-$Zn_xMnO_2{\cdot}nH_2O$ during the initial discharging process. After following the cycling processes, Zn^{2+} was reversibly (de)intercalated into the H_2O-containing Zn-buserite framework[116]. In addition, conversion reaction based on the formation of the intermediate product of MnOOH, triggered by H insertion into cathode lattice during discharge/charge process, has been proposed, as shown in Fig.8(B)[117]. In most cases, the conversion reaction is usually accompanied with reversible (de)intercalation of Zn and H ions. Hence, the well-utilization of both conversion and intercalation mechanisms holds significant promise for the development of high-performance AZIBs.

4.3 Dissolution-deposition Mechanism

Besides the above-mentioned energy storage mechanisms, the dissolution-deposition mechanism has been proposed and considered as a novel redox chemistry based on a two-electron transfer reaction. The specific mechanism has been demonstrated by producing Mn^{2+} *via* the reaction between α-MnO_2 and water in the initial discharge process[118]. Then, the resultant OH^- reacted with SO_4^{2-} and Zn^{2+} in $ZnSO_4$ electrolyte, forming the flaky zinc sulfate hydroxide(ZSH) on the cathode surface. Upon recharging, the ZSH phase reacted with the dissolved Mn^{2+} in an electrolyte to form birnessite-MnO_2. During the following cycles, reversible electrolytic reactions involving dissolution and deposition took place with the birnessite-MnO_2 rather than the initial phase of α-MnO_2. In order to explore the dissolution-deposition mechanism, Bao *et al.*[119] synthesized ZSH as a cathode material to directly verify the phase transition of MnO_2 during the cycling tests. As a result, the synthesized ZSH exhibited similar electrochemical reaction behavior with α-MnO_2 and δ-MnO_2. Moreover, a series of electrochemical characterizations confirmed that the two-electron solid-liquid reaction of MnO_2/Mn^{2+} can be accompanied by reversible dissolution-deposition of the ZSH flakes in Fig.8(C).

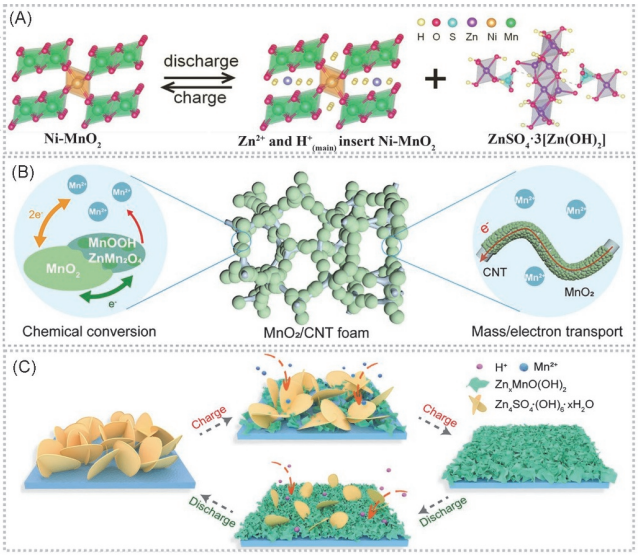

Fig.8 Schematic diagrams of energy storage mechanism in MnO_2 cathodes

(A) Mechanism of Zn^{2+} and H^+ co-insertion in MnO_2 electrodes; (B) MnO_2/CNT foam cathode features chemical conversion reaction mechanism; (C) ZSH-assisted deposition−dissolution mechanism for two-electron transfer reaction. (A) Reprinted with permission form Ref.[73], Copyright 2022, Wiley-VCH; (B) reprinted with permission from Ref.[117], Copyright 2021, Wiley-VCH; (C) reprinted with permission from Ref.[119], Copyright 2022, Wiley-VCH.

https://doi.org/10.1007/s40242-023-3126-x

Recently, Zhou *et al.*[120] introduced acetate into the electrolyte to enhance the stability of MnO_2, in which Ac^- can indirectly increase the redox potential of Zn-MnO_2 batteries through adjustment of the coordination environment, as shown in Fig.9(A). Besides, the Cr^{3+}/Cr^{2+} redox couple was introduced into battery system to catalyze the Mn^{4+}/Mn^{2+} redox reaction based on dissolution-deposition mechanism, eliminating extra electrochemical "dead" MnO_2 and contributing to a long lifespan. Similarly, the Fe^{3+}/Fe^{2+} redox species have been proven as a redox mediator to accelerate dissolution-deposition reaction of MnO_2/Mn^{2+}[121]. During the discharge process, Fe^{3+} underwent electrochemical reduction to form Fe^{2+}. Furthermore, the resulting Fe^{2+} species promoted the conversion of Mn^{3+} and MnO_2 into Mn^{2+}, while Fe^{2+} was re-oxidized back to Fe^{3+}. Finally, two electron transfer of MnO_2/Mn^{2+} can eventually be realized accompanied by the redox couple of Fe^{3+}/Fe^{2+}, as shown in Fig.9(B). Recently, Chao *et al.*[122] proposed that the pH environment or proton reactivity could tune the occurrence of energy storage mechanisms, which typically coexist and evolve alternately. So another way to benefit the dissolution/deposition of MnO_2 cathode is by lowering the pH value of the electrolyte, in other words, to achieve two-electron transfer system. Therefore, a continuous and in-depth investigation into the dissolution-deposition mechanism can open an avenue for constructing high-performance Zn-Mn batteries based on multi electron transfer reactions.

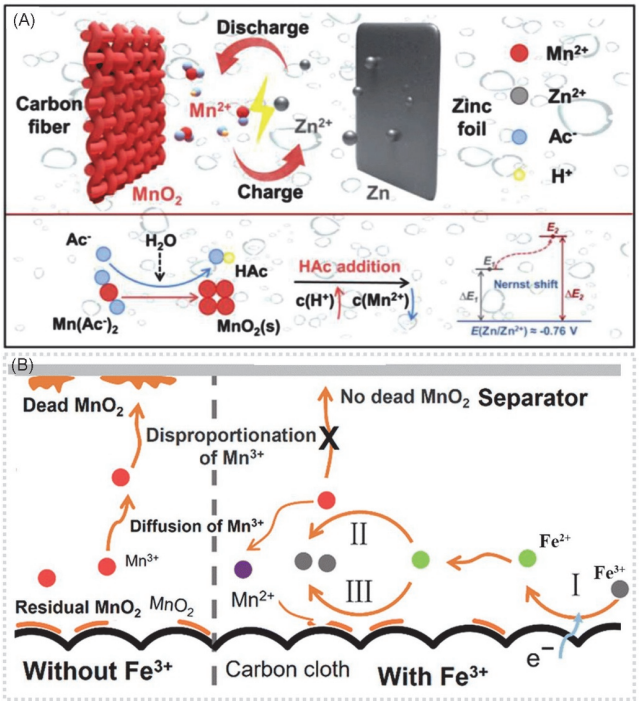

Fig.9 Electrolyte modification for boosting deposition-dissolution mechanism

(A) Schematic of acetate-based Zn-MnO_2 battery through coordination reaction adsorbing Mn^{3+}; (B) schematic of the formation of "dead" MnO_2 and the working mechanisms of Fe^{3+}/Fe^{2+} redox couple for inhibiting the reaction of disproportionation of Mn^{3+}.

(A) Reprinted with permission from Ref.[120], Copyright 2022, Elsevier; (B) reprinted with permission from Ref.[121], Copyright 2023, Royal Society of Chemistry.

5 Challenges and Prospects

High performance aqueous Zn-MnO_2 batteries have significant potential for large-scale energy storage applications. However, Zn batteries still face the main pitfalls of unsatisfying energy density and cycling stability. Although great progress has been achieved in recent years, many issues still need to be addressed for the commercialization of advanced Zn-MnO_2 batteries. Holistic improvement of the electrodes and electrolytes can achieve the overall high-performance Zn devices. Hence, continuous optimization of the electrochemical performance of AZIBs is the exploration target. Herein, we conclude some challenges and prospects based on these issues, as shown in Fig.10.

(1) Rational design of nanostructured MnO_2. Structural engineering is effective for the conductivity, zinc ion storage, and stability of MnO_2 cathodes. Nevertheless, an in-depth study of the mechanisms in the enhanced performance is still unclear. So, the *in-situ* characterizations can be used for the comprehensive study. Except for a simple strategy of ion doping or pre-intercalation, introducing multiple redox couples can effectively increase the electron transfer number for high-capacity Mn-based cathodes. Furthermore, novel organics with flexible molecular chains and functional groups might act as "guest materials" to enhance organic-inorganic cathodes integrity and reaction kinetics.

(2) Systematic study of energy storage mechanism. The redox chemistry of Zn-MnO_2 devices still lacks recognized mechanism. Hence, advanced technologies and DFT

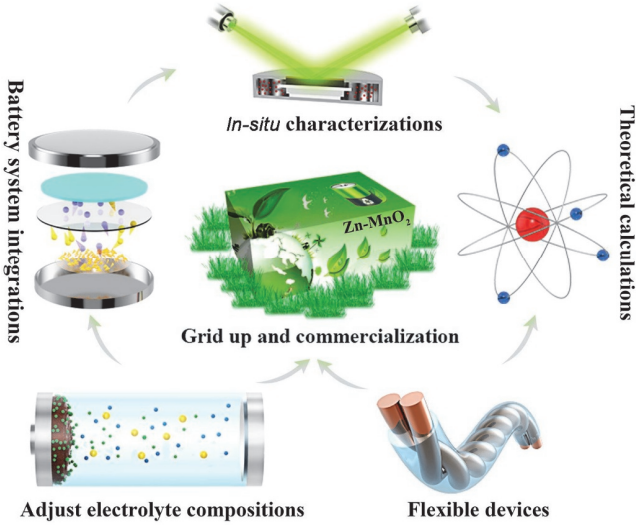

Fig.10 Future challenges and prospects of advanced Zn-MnO_2 batteries for large-scale energy storage applications

calculation are utilized to explore the reaction process prediction of Mn-based Zn batteries. For example, the application of advanced *in-situ* characterizations and DFT calculation are employed for the structure-function relationship of the modified cathodes and various electrochemical properties. Furthermore, high throughput DFT simulation can predict reliable Mn-based hosts according to the relevant database and clear redox chemistry.

(3) Composition optimization of electrolyte. Dissolution-deposition mechanism of MnO_2/Mn^{2+} features excellent theoretical specific capacity(616 $mA{\cdot}h{\cdot}g^{-1}$) and high discharge working voltage, which has been implemented for superb Zn devices. To avoid the strong corrosions of Zn anodes in acid electrolytes, introducing new redox couples, such as Fe^{3+}/Fe^{2+}, Cr^{3+}/Cr^{2+} and I^-/I_3^- into the weak acid electrolyte is a good choice for increasing ion storage sites. In addition, replacing the traditional sulfate electrolyte with an acetate electrolyte can effectively catalyze the reversible dissolution-deposition reaction. Moreover, rate performance and stability of the battery effectively can be improved through the complexation of Ac^- and the inhibited disproportionation of Mn^{3+}[120]. Besides, eutectic mixtures have been developed quickly, in last years, as a green, safe, cheap-cost and electrochemically stable electrolyte for AZIBs, which can stable the electrochemical window and electrode/electrolyte interfaces to boost charge transfer kinetics[123,124]. Therefore, attentions should be focused on improving the dynamics and reversibility of the relevant multi-electron reactions *via* electrolyte optimization, which offers significant benefits for future Zn-Mn industries[125,126].

(4) Protection strategies of Zn anodes. Besides reasonable modification of MnO_2 materials and electrolytes, the protection of zinc anodes should also be considered. Zn anodes mainly face the issues of dendrite growth, hydrogen evolution, and enhanced internal pressure of a sealed cell, which seriously hinder the development of AZIBs for large-scale energy storage systems[127]. Tailoring structures and adjusting compositions of Zn anodes are all effective methods for improving the reversibility and stability of AZIBs. Additionally, *in situ* modification process that forms the solid electrolyte interface(SEI) on the metallic Zn deserves close attention[128]. Specifically, coating functionalized layers of active carbon, porous TiO_2 and polymers can effectively decrease the polarization and dendrite growth, and enhance the interfacial stability, simultaneously. Hence, more efforts are required to overcome the issues faced by Zn anodes.

(5) Flexible devices in practical application. AZIBs show promise for using as flexible batteries with the advantages of intrinsic safety and low cost. Solid or gel electrolytes might be matched with a modified MnO_2 cathode and a Zn anode for the flexible Zn batteries. Due to the characteristics of high mechanical strength, good ductility and good machinability, solid/gel polymer electrolyte has broad application prospects in future intelligent, flexible and wear-resistant fields. The application of Mn-based Zn devices is prevented by the inferior conductivity and low areal capacity of deposited MnO_2, which can be regulated by adjusting the deposited temperature and polymorph tuning method[129]. For the large-scale energy storage, the overall integration of cathode/anode ratio, electrolyte usage and cost considerations must be studied. Therefore, the development of simple methods for high energy density and long lifespan of Zn-MnO_2 batteries is very necessary for its commercialization.

Acknowledgements

This work was supported by the National Natural Science Foundation of China (Nos.22209006, 21935001), the Natural Science Foundation of Shandong Province, China(No.ZR2022QE009), the Fundamental Research Funds for the Central Universities of China(No.buctrc202307) and the Key Beijing Natural Science Foundation, China(No.Z210016).

We also thank the Ministry of Finance and the Ministry of Education of China for long-term subsidy mechanism.

Conflicts of Interest

The authors declare no conflicts of interest.

References

[1] Suo L. M., Borodin O., Sun W., Fan X. L., Yang C. Y., Wang F., Gao T., Ma Z. H., Schroeder M., Von Cresce A., Russell S. M., Armand M., Angell A., Xu K., Wang C. S., *Angew. Chem. Int. Ed.*, **2016**, *128*(25), 7252

[2] Wang F., Suo L. M., Liang Y. J., Yang C. Y., Han F. D., Gao T., Sun W., Wang C. S., *Adv. Energy Mater.*, **2016**, *7*(8), 1600922

[3] Fang G. Z., Zhou J., Pan A. Q., Liang S. Q., *ACS Energy Lett.*, **2018**, *3*(10), 2480

[4] Liu N., Wu X., Fan L., Gong S., Guo Z., Chen A., Zhao C., Mao Y., Zhang N., Sun K., *Adv. Mater.*, **2020**, *32*(42), e1908420

[5] Wang S., Yuan Z., Zhang X., Bi S. S., Zhou Z., Tian J. L., Zhang Q. C., Niu Z. Q., *Angew. Chem. Int. Ed.*, **2021**, *60*(13), 7056

[6] Tang H., Chen W. H., Li N., Hu Z. L., Xiao L., Xie Y. J., Xi L. J., Ni L., Zhu Y. R., *Energy Storage Mater.*, **2022**, *48*, 335

[7] Shi X., Liu X. Y., Wang E. Z., Cao X. S., Yu Y. X., Cheng X. N., Lu X. H., *Carbon Neutralization*, **2022**, *2*(1), 28

[8] Guo S., Liang S., Zhang B. S., Fang G. Z., Ma D., Zhou J., *ACS Nano*, **2019**, *13*(11), 13456

[9] Zhang K., Han X., Hu Z., Zhang X. L., Tao Z. L., Chen J., *Chem. Soc. Rev.*, **2015**, *44*(3), 699

[10] Xiong T., Yu Z. G., Wu H. J., Du Y. H., Xie Q. D., Chen J. S., Zhang Y. W., Pennycook S. J., Lee W. S. V., Xue J. M., *Adv. Energy Mater.*, **2019**, *9*(14), 1803815

[11] Xiong T., Zhang Y. X., Lee W. S. V., Xue J. M., *Adv. Energy Mater.*, **2020**, *10*(34), 2001769

[12] Huang J., Tang X., Liu K., Fang G., He Z., Li Z., *Mater. Today Energy*, **2020**, *17*, 100475

[13] Zhao Q. H., Song A. Y., Ding S. X., Qin R. Z., Cui Y. H., Li S. N., Pan F., *Adv. Mater.*, **2020**, *32*(50), 2002450

[14] Zhang Y., Yuan C. L., Ye K., Jiang X., Yin J. L., Wang. G. L., Cao D. X., *Electrochim. Acta*, **2014**, *148*, 237

[15] Zhang Y., Deng S., Luo M., Pan G., Zeng Y., Lu X., Ai C., Liu Q., Xiong Q., Wang X., Xia X., Tu J., *Small*, **2019**, *15*(47), e1905452

[16] Wei C. G., Xu C. J., Li B. H., Du H. D., Kang F. Y., *J. Phys. Chem. Solids*, **2012**, *73*(12), 1487

[17] Wang Y., Huo W. C., Yuan X. Y., Zhang Y. X., *Acta Mech. Solida Sin.*, **2020**, *36*(2), 1904007

[18] Tang Y. J., Zheng S. S., Xu Y. X., Xiao X., Xue H. G., Pang H., *Energy Storage Mater.*, **2018**, *12*, 284

[19] Zhang N., Cheng F. Y., Liu J., Wang L., Long X., Liu X., Li F., Chen J., *Nat. Commun.*, **2017**, *8*(1), 405

[20] Lee B., Lee H. R., Kim H., Chung K. Y., Cho B. W., Oh S. H., *Chem. Commun.*, **2015**, *51*(45), 9265

[21] Lian S. T., Sun C. L., Xu W. N., Huo W. C., Luo Y. Z., Zhao K. N., Yao G.,

Xu W. W., Zhang Y. X., Li Z., Yu K. S., Zhao H. B., Cheng H. W., Zhang J. J., Mai L. Q., *Nano Energy*, **2019**, *62*, 79
[22] Song M., Tan H., Chao D. L., Fan H. J., *Adv. Funct. Mater.,* **2018**, *28*(41), 1802564
[23] Shi W., Lee W. S. V., Xue J., *ChemSusChem,* **2021**, *14*(7), 1634
[24] Yuan C. L., Zhang Y., Pan Y., Liu X. W., Wang G. L., Cao D. X., *Electrochim. Acta,* **2014**, *116*, 404
[25] Housel L. M., Wang L., Abraham A., Huang J., Renderos G. D., Quilty C. D., Brady A. B., Marschilok A. C., Takeuchi K. J., Takeuchi E. S., *Acc. Chem. Res.,* **2018**, *51*(3), 575
[26] Li X., Li Y., Xie S. Y., Zhou Y. J., Rong J. H., Dong L. B., *Chem. Eng. J.,* **2022**, *427*, 131799
[27] Sambandam B., Mathew V., Kim S., Lee S., Kim S., Hwang J. Y., Fan H. J., Kim J., *Chem,* **2022**, *8*(4), 924
[28] Cheng F. Y., Zhao J. Z., Song W. E., Li C. S., Ma H., J H., Chen J., Shen P. W., *Inorganic Chemistry,* **2006**, *45*, 2038
[29] Han M., Huang J., Liang S., Shan L., Xie X., Yi Z., Wang Y., Guo S., Zhou J., *iScience,* **2020**, *23*(1), 100797
[30] Cheng F. Y., Chen J., Gou X. L., Shen P. W., *Adv. Mater.,* **2005**, *17*, 2753
[31] Hu X., Han X., Hu Y., Cheng F., Chen J., *Nanoscale,* **2014**, *6*(7), 3522
[32] Liu G. X., Huang H. W., Bi R., Xiao X., Ma T. Y., Zhang L., *J. Mater. Chem. A,* **2019**, *7*, 20806
[33] Shang P., Liu Y. H., Mei Y. Y., Wu L. S., Dong Y. F., *Mater. Chem. Front.,* **2021**, *5*(22), 8002
[34] Zhao Y. L., Zhu Y. H., Zhang X. B., *InfoMat.,* **2019**, *2*(2), 237
[35] Wang X., Zhang Z. C. Y., Xi B. J., Chen W. H., Jia Y. X., Feng J. K., Xiong S. L., *ACS Nano,* **2021**, *15*(6), 9244
[36] Chen D., Lu M. J., Cai D., Yang H., Han W., *J. Energy Chem.,* **2021**, *54*, 712
[37] Grocker A. G., *Experimental Mechanics Volume,* **1996**, *6*, 266
[38] Pinaud B. A., Chen Z. B., Abram D. N., Jaramillo T. F., *J. Phys. Chem. C,* **2011**, *115*(23), 11830
[39] John R. E., Chandran A., Thomas M., Jose J., George K. C., *Appl. Surf. Sci.,* **2016**, *367*, 43
[40] Cheng F. Y., Zhang T. R., Zhang Y., Du J., Han X. P., Chen J., *Angew. Chem. Int. Ed.,* **2013**, *52*(9), 2474
[41] Xiong T., Yu Z. G., Wu H. J., Du Y. H., Xie Q. D., Chen J. S., Zhang Y. W., Pennycook S. J., Lee W. S. V., Xue J. M., *Adv. Energy Mater.,* **2019**, *9*(14), 1803815
[42] Zhao Y. J., Zhang P. J., Liang J. R., Xia X. Y., Ren L. T., Song L., Liu W., Sun X. M., *Energy Storage Mater.,* **2022**, *47*, 424
[43] Xie S., Li X., Li Y., Liang Q. H., Dong L. B., *Chem. Rec.,* **2022**, *22*(10), e202200201
[44] Li Y., Li X., Duan H., Xie S. Y., Dai R. Y., Rong J. H., Kang F. Y., Dong L. B., *Chem. Eng. J.*, **2022**, *441*, 136008
[45] Gao P., Chen Z., Gong Y. X., Zhang R., Liu H., Tang P., Chen X. H., Passerini S., Liu J. L., *Adv. Energy Mater.,* **2020**, *10*(14), 1903780
[46] Chao D., Zhou W., Ye C., Zhang Q., Chen Y., Gu L., Davey K., Qiao S. Z., *Angew. Chem. Int. Ed.,* **2019**, *58*(23), 7823
[47] Zhang Y. N., Liu Y. P., Liu Z. H., Wu X. G., Wen Y. X., Chen H. D., Ni X., Liu G. H., Huang J. J., Peng S. L., *J. Energy Chem.,* **2022**, *64*, 23
[48] Zhao M., Luo Y., Zhu L., Cai D., Zhuang Y., Chen Q., Zhan H., *Alloy Compd.,* **2022**, *913*, 165124
[49] Kim S., Koo B., Jo Y., An H., Lee Y., Huang C., An G., *J. Mater. Chem. A,* **2021**, *9*(32), 17211
[50] Ge B. C., Sun Y., Guo J. X., Yan X. B., Fernandez C., Peng Q. M., *Small,* **2019**, *15*(34), 1902220
[51] Yan L. J., Niu L. Y., Shen C., Zhang Z. K., Lin J. H., Shen F. Y., Gong Y. Y., Li C., Liu X. J., Q. X. S., *Electrochim. Acta,* **2019**, *306*, 529
[52] Ye Z. G., Li T., Ma G., Dong Y. H., Zhou X. L., *Adv. Funct. Mater.,* **2017**, *27*(44), 1704083
[53] Zhao Y. F., Zhang J. Q., Wu W. J., Guo X., Xiong P., Liu H., Wang G. X., *Nano Energy,* **2018**, *54*, 129
[54] Ji J., Wan H. Z., Zhang B., Wang C., Gan Y., Tan Q. Y., Wang N. Z., Yao J., Zheng Z. H., Liang P., Zhang J., Wang H. B., Tao L., Wang Y., Chao D. L., H. W., *Adv. Energy Mater.,* **2020**, *11*, 2003203
[55] Xia X. Y., Zhao Y. J., Zhao Y., Xu M. G., Liu W., Sun X. M., *Nano Res.,* **2022**, *16*(2), 2511
[56] Wang C. Z., Yang H., Wang B., Ding P. B., Wan Y., Bao W. J., Li Y. A., Ma S. Y., Liu Y., Lu Y. K., Hu H., *Nano Res.,* **2023**, doi:10.1007/s12274-023-5717-8
[57] Selvakumaran D., Pan A. Q., Liang S. Q., Cao G. Z., *J. Mater. Chem. A,* **2019**, *7*(31), 18209
[58] Bi S., Wu Y., Cao A., Tian J., Zhang S., Niu Z., *Mater. Today Energy,* **2020**, *18*, 100548
[59] Li B., Chai J. W., Ge X. M., An T., Lim P., Liu Z. L., Zong Y., *ChemNanoMat,* **2017**, *3*(6), 401
[60] Xu D. W., Li B. H., Wei C. G., He Y. B., Du H. D., Chu X. D., Qin X. Y., Yang Q. H., Kang F. Y., *Electrochim. Acta,* **2014**, *133*, 254
[61] Khamsanga S., Pornprasertsuk R., Yonezawa T., Mohamad A. A., Kheawhom S., *Sci. Rep.,* **2019**, *9*(1), 8441
[62] Wang C., Zeng Y. X., Xiao X., Wu S. J., Zhong G. B., Xu K. Q., Wei Z. F., Su W., Lu X. H., *J. Energy Chem.,* **2020**, *43*, 182
[63] Li C., Li M., Xu H., Zhao F., Gong S., Wang H., Qi J., Wang Z., Hu Y., Peng W., Fan X., Liu J., *J. Colloid Interface Sci.,* **2022**, *628*(Pt A), 553
[64] Jeong J., Park S. H., Park H. J., Jin S. B., Son S. G., Moon J., Suh H., Choi B. G., *Adv. Funct. Mater.,* **2021**, *31*(17), 2009632
[65] Jia H. N., Lin J. H., Liu Y. L., Chen S. L., Cai Y. F., Qi J. L., Feng J. C., Fei W. D., *J. Mater. Chem. A,* **2017**, *5*(21), 10678
[66] Ataherian F., Wang Y. L., Tabet-Aoul A., Mohamedi M., *ChemElectroChem,* **2017**, *4*(8), 1924
[67] Sheng L. Z., Jiang L. L., Wei T., Fan Z. J., *Small,* **2016**, *12*(37), 5217
[68] Tong H., Li T., Liu J., Gong D., Xiao J., Shen L., Ding B., Zhang X., *Energy Technol.*, **2020**, *9*(2), 2000769
[69] Chao D. L., Zhou W. H., Ye C., Zhang Q. H., Chen Y. G., Gu L., Davey K., Qiao S. Z., *Angew. Chem. Int. Ed.,* **2019**, *58*(23), 7823
[70] Huang C., Wang Q. F., Tian G. F., Zhang D. H., *Mater. Today Phys.,* **2021**, *21*, 100518
[71] Zhang J., Lin J., Zeng Y. B., Zhang Y., Guo H., *ACS Appl. Energy Mater.,* **2019**, *2*(11), 8345
[72] Zhao Y., Zhou R. K., Song Z. H., Zhang X. D., Zhang T., Zhou A. B., Wu F., Chen R. J., Li L., *Angew. Chem. Int. Ed.,* **2022**, *61*(49), e202212231
[73] Ji J., Yao J., Xu Y. C., Wan H. Z., Zhang B., Lv L., Li J. Y., Wang N. Z., Zheng Z. H., Zhang J., Ma G. K., Tao L., Wang H. B., Wang Y., Wang H., *Energy Environ. Sci.,* **2022**, *6*(2), e12340
[74] Sun Y. K., Lee M. J., Yoon C. S., Hassoun J., Amine K., Scrosati B., *Adv. Mater.,* **2012**, *24*(9), 1192
[75] Jung Y. S., Cavabagh A. S., Riley L. A., Kang S. H., Dillon A. C., Groner M. D., Groner S. M., Lee S. H., *Adv. Mater.,* **2010**, *22*(19), 2172
[76] Liu Y., Zhou X. M., Liu R., Li X. L., Bai Y., Xiao H. H., Wang, Y. M., Yuan G. H., *ACS Appl. Mater. Interfaces,* **2019**, *11*(21), 19191
[77] Li H. Y., Yao H., Sun X. Y., Sheng C. C., Zhao W., Wu J. H., Chu S. Y., Liu Z. G., Guo S. H., Zhou H. S., *Chem. Eng. J.,* **2022**, *446*, 137205
[78] Ruan P. C., Xu X. L., Gao X. L., Feng J. X., Yu L. H., Cai Y. H., Gao X. B., Shi W. H., Wu F. F., Liu W. X., Zang X. X., Ma F. Y., Cao X. H., *SM&T,* **2021**, *28*, e00254
[79] Yao X. H., Zhao Y. L., Castro F. A., Mai L. Q., *ACS Energy Lett.,* **2019**, *4*(3), 771
[80] Xia H., Zhu X. H., Liu J. Z., Liu Q., Lan S., Zhang Q. H., Liu X. Y., Seo J. K., Chen T. T., Gu L., Meng Y. S., *Nat. Commun.,* **2018**, *9*(1), 5100
[81] Ye Q. L., Dong R. T., Xia Z. H., Chen G. R., Wang H. L.,Tan G. J., Jiang L., Wang F., *Electrochim. Acta,* **2014**, *141*, 286
[82] Zhang K. Q., Chen H. D., Xiao B. Q., Chen J., Yan W., Liu Y. P., Hu C. F., Chen L., Huang J. J., Peng S. L., *ACS Appl. Mater. Interfaces,* **2023**, *6*(3), 1467
[83] Yadav G. G., Gallaway J. W., Turney D. E., Nyce M., Huang J., Wei X., Banerjee S., *Nat. Commun.,* **2017**, *8*, 14424
[84] Long F., Xiang Y., Yang S., Li Y., Du H., Liu Y., Wu X., Wu X., *J. Colloid Interface Sci.,* **2022**, *616*, 101
[85] Poyraz A. S., Huang J. P., Pelliccione C. J., Tong X., Cheng S. B., Wu L. J., Zhu Y. M., Marschilok A. C., Takeuchi K. J., Takeuchi E. S., *J. Mater. Chem. A,* **2017**, *5*(32), 16914
[86] Sada K., Senthilkumar B., Barpanda P., *J. Mater. Chem. A,* **2019**, *7*(41), 23981
[87] Radhamani A. V., Krishna Surendra M., Ramachandra Rao M. S., *Appl. Surf. Sci.,* **2018**, *450*, 209
[88] Zhai X. Z., Qu J., Hao S. M., Jing Y. Q., Chang W., Wang J., Li W., Abdelkrim Y., Yuan H., Yu Z. Z., *Nano-Micro Lett.,* **2020**, *12*(1), 56
[89] Liu L. Y., Wu Y., Huang L., Liu K. S., Duployer B., Rozier P., Taberna P., Simon P., *Adv. Energy Mater.,* **2021**, *11*(31), 2101287
[90] Liu Z. X., Sun H. M., Qin L. P., Cao X. X., Zhou J., Pan A. Q., Fang G. Z., Liang S. Q., *ChemNanoMat,* **2020**, *6*(11), 1553
[91] Jiao Y. D., Kang L. Q., Berry-Gair J., McCol K., Li J. W., Dong H. B., Jiang H., Corà F., Brett D. J. L., He G. J., Parkin I. P., *J. Mater. Chem. A,* **2020**, *8*(42), 22075
[92] Chen C., Shi M. J., Zhao Y., Yang C., Zhao L. P., Yan C., *Chem. Eng. J.,* **2021**, *422*, 130375
[93] Zhao X., Mao L., Cheng Q. H., Liao F. F., Yang G. Y., Lu X. H., Chen L. Y., *Energy Storage Mater.,* **2021**, *38*, 397
[94] Lu Y. Y., Zhu T. Y., Bergh W. V. D., Stefik M., Huang K., *Angew. Chem. Int. Ed.,* **2020**, *59*(39), 17004
[95] Wei X., Peng Z., Mao X. H., Wang D. H., *J. Mater. Chem. A,* **2015**, *3*, 8676
[96] Huang J. H., Wang Z., Hou M. Y., Dong X. L., Liu Y., Wang Y. G., Xia Y. Y., *Nat. Commun.,* **2018**, *9*(1), 2906
[97] Chen H., Ma W. B., Guo J. D., Xiong J. Y., Hou F., Si W. P., Sang Z. Y., Yang D., *J. Alloys Compd.,* **2023**, *932*, 167688

[98] Liao X. B., Pan C. L., Pan Y. S., Yin C. J., *J. Alloys Compd.,* **2021**, *888*, 161619
[99] Zhao Q., Huang W., Luo Z., Liu L., Lu Y., Li Y., Li L., Hu J., Ma H., Chen J., *Sci. Adv.,* **2018**, *4*(3), aao1761
[100] Nam K. W., Kim H., Beldjoudi Y., Kwon T., Kim D. J., Stoddart J. F., *J. Am. Chem. Soc.,* **2020**, *142*(5), 2541
[101] Sun T., Li Z. J., Zhi Y. F., Huang Y. J., Fan H. J., Zhang Q. C., *Adv. Funct. Mater.,* **2021**, *31*(16), 2010049
[102] Lin Z., Shi H. Y., Lin L., Yang X., Wu W., Sun X., *Nat. Commun.,* **2021**, *12*(1), 4424
[103] Tie Z. W., Niu Z. Q., *Angew. Chem. Int. Ed.,* **2020**, *59*(48), 21293
[104] Gao Y. J., Li G. F., Wang F., Chu J., Yu P., Wang B. S., Zhan H., Song Z. P., *Energy Storage Mater.,* **2021**, *40*, 31
[105] Wang Y., Wang C., Ni Z., Gu Y., Wang B., Guo Z., Wang Z., Bin D., Ma J., Wang Y., *Adv. Mater.,* **2020**, *32*(16), e2000338
[106] Wu X. Y., Hong J. J., Shin W., Ma L., Liu T. C., Bi X. X., Yuan Y. F., Qi Y. T., Surta T. W., Huang W. X., Neuefeind J., Wu T. P., Greaney P. A., Lu J., Ji X. L., *Nat. Energy,* **2019**, *4*(2), 123
[107] Yang X., Zhao Y., Xu Q. J., Yuan X. C., Liu J. Z., *Batteries & Supercaps,* **2023**, *6*(3), e202200480
[108] Ye F., Liu Q., Lu C. J., Meng F. Q., Lin T., Dong H. L., Gu L., Wu Y. P., Tang Z. L., Hu L. F., *Energy Storage Mater.,* **2022**, *52*, 675
[109] Lee B., Yoon C. S., Lee H. R., Chung K. Y., Cho B. W., Oh S. H., *Sci. Rep.,* **2014**, *4*, 6066
[110] Sun W., Wang F., Hou S., Yang C., Fan X., Ma Z., Gao T., Han F., Hu R., Zhu M., Wang C., *J. Am. Chem. Soc.,* **2017**, *139*(29), 9775
[111] Xu C. J., Li B. H., Du H. D., Kang F. Y., *Angew. Chem. Int. Ed.,* **2012**, *51*(4), 933
[112] Lee J., Ju J. B., Cho W. I., Cho B. W., Oh S. H., *Electrochim. Acta,* **2013**, *112*, 138
[113] Alfaruqi M. H., Gim J., Kim S., Song J. J., Jo J., Kim S., Mathew V., Kim J., *J. Power Sources,* **2015**, *288*, 320
[114] Zhang N., Cheng F. Y., Liu Y. C., Zhao Q., Lei K. X., Chen C. C., Liu X. S., Chen J., *J. Am. Chem. Soc.,* **2016**, *138*(39), 12894
[115] Islam S., Alfaruqi M. H., Mathew V., Song J. J., Kim S., Kim S., Jo J., Baboo J. P., Pham D. T., Putro D. Y., Sun Y. K., Kim J., *J. Mater. Chem. A,* **2017**, *5*(44), 23299
[116] Zeng Y., Zhang X., Meng Y., Yu M., Yi J., Wu Y., Lu X., Tong Y., *Adv. Mater.,* **2017**, *29*(26), 1700274
[117] Shen X. F., Wang X. N., Zhou Y. R., Shi Y. H., Zhao L. M., Jin H. H., Di J. T., Li Q. W., *Adv. Funct. Mater.,* **2021**, *31*(27), 2101579
[118] Guo X., Zhou J., Bai C. L., Li X. K., Fang G. Z., Liang S. Q., *Mater. Today Energy,* **2020**, *16*, 100369
[119] Chen H., Dai C. L., Xiao F. Y., Yang Q. J., Cai S. N., Xu M. W., Fan H. J., Bao S. J., *Adv. Mater.,* **2022**, *34*(15), 2109092
[120] Liu Z. X., Yang Y. Q., Lu B. G., Liang S. Q., Fan H. J., Zhou J., *Energy Storage Mater.,* **2022**, *52*, 104
[121] Ye X. L., Han D. L., Jiang G. Y., Cui C. J., Guo Y., Wang Y. G., Zhang Z. C., Weng Z., Yang Q. H., *Energy Environ. Sci.,* **2023**, *16*(3), 1016
[122] Yang H., Zhang T., Chen D., Tan Y., Zhou W., Li L., Li W., Li G., Han W., Fan H. J., Chao D., *Adv. Mater.,* **2023**, *35*(24), e2300053
[123] Han M., Zhou J., Fan H. J., *Trends in Chemistry,* **2023**, *5*(3), 214
[124] Li C., Kingsbury R., Thind A. S., Shyamsunder A., Fister T. T., Klie R. F., Persson K. A., Nazar L. F., *Nat. Commun.,* **2023**, *14*(1), 3067
[125] Chen D., Lu M. J., Wang B., Cheng H. F., Yang H., Cai D., Han W., Fan H. J., *Nano Energy,* **2021**, *83*, 105835
[126] Wang Y., Xie J. H., Luo J., Yu Y. X., Liu X. Q., Lu X. H., *Small Methods,* **2022**, *6*(8), e2200560
[127] Zhang C., Holoubek J., Wu X., Daniyar A., Zhu L., Chen C., Leonard D. P., Rodriguez-Perez I. A., Jiang J. X., Fang C., Ji X., *Chem. Commun. (Camb),* **2018**, *54*(100), 14097
[128] Zhang N., Chen X., Yu M., Niu Z., Cheng F., Chen J., *Chem. Soc. Rev.,* **2020**, *49*(13), 4203
[129] Xiao X., Zhang Z., Wu Y., Xu J., Gao X., Xu R., Huang W., Ye Y., Oyakhire S. T., Zhang P., Chen B., Cevik E., Asiri S. M., Bozkurt A., Amine K., Cui Y., *Adv. Mater.,* **2023**, e2211555, https://doi.org/10.1002/adma.202211555